Analysis of Measurement Tidal Type of Musi River

Febriansyah[1], Erika Buchari[1] ⓘ*, Edi Kadarsa[1]
[1]Department of Civil Engineering, Faculty of Engineering
Sriwijaya University, Palembang, Indonesia
Correspondence Email: erikabuchari@ ft.unsri.ac.id
ORCID ID: 0000-0002-4278-0514

ARTICLE INFORMATION

ABSTRACT

Along the Musi River, there are transportation activities involving both passenger and cargo transport. However, all these activities are affected by the Musi River's tidal fluctuations. Cargo transport on the Musi River is heavily dependent on the tidal conditions. The dimensions of the ships operating in the Musi River are determined by the river's depth, which is influenced by these tidal changes. Consequently, the draft of the vessel that can operate is limited by the prevailing depth conditions of the river. This study aims to identify the highest and lowest tidal levels in the Musi River, determine the tidal pattern type, and forecast tidal conditions for December 2026. The methodology employed in this research is the Admiralty Method, which is based on observational data collected over 29 days, ensuring high accuracy in the results. From the research findings, the highest tide reached 551 cm, while the lowest tide recorded was 215 cm, resulting in a tidal range of 336 cm. The type of tidal pattern observed in the Musi River is classified as a mixed prevailing diurnal type, with a HHWL of 557.71 cm, a MSL of 364.5 cm, and a LLWL of 171.26 cm. Based on the tidal forecast for December 2026, the highest tide is projected at 511.1 cm, while the lowest is 219.3 cm, resulting in a tidal range of 291.9 cm. This research is anticipated to provide valuable insights into determining safe ship dimensions for navigation on the Musi River.

Keywords: HHWL; River Transportation; Tide; Tidal Prediction; Tidal Type

INTRODUCTION

Tidal fluctuations have long disrupted shipping on the Musi River. The dimensions of the ships operating in the Musi River depend on the river's depth, which is influenced by these tidal changes. Consequently, the draft of the vessel is limited by the prevailing depth conditions of the river. Generally, river transport activities are affected by tidal fluctuations. However, with the implementation of water-level management technologies used on the Meuse River, tidal fluctuations need not pose a significant challenge to navigation (Patil et al., 2024). It is essential to maintain navigational channel conditions, such as depth, to ensure that river activities can continue uninterrupted (Bedulkis et al., 2023).

In the context of river transport, rivers serve as the primary infrastructure for shipping. River navigability is influenced by factors such as depth (Fathoni et al., 2020). At the estuary of the Musi River, tidal variations can reach up to 3.3 meters, meaning ships may not be able to pass through specific points in the river at all times (Sulistiyani et al., 2019). Additionally, sedimentation occurs at a rate of 40 cm per month, limiting the operation of larger draft ships in the port (Putranto & Buchari, 2017).

Tidal fluctuations in rivers are influenced by the regional geography (Wei et al., 2016) and the gravitational effects of the moon and the sun (Finkl & Makowski, 2019). In planning river transportation activities, tidal data is essential. This data can support transportation activities (Lima et al., 2024), regional planning (Rusdin, 2024), and disaster mitigation (Adalya & Mutaqin, 2022; Isnain & Mutaqin, 2023). Tides significantly affect regional development, especially in areas that rely solely on river transportation.

Changes in water levels affect the draft of ships and the height at which ships can navigate through the river. During high tide, ships can safely navigate the river; however, during low tide, river activities may be disrupted (Khedr, 2024). The type of tide influences waterborne activities, such as port operations. Port activities may experience changes in service times and shipping routes due to tidal variations (Rusdin & Yanuar, 2024), which can also affect transportation costs (Pasaribu et al., 2022). Therefore, it is crucial for navigators to interpret tidal changes (Mustain, 2021) accurately. Additionally, fluctuations in sea level can affect tidal patterns in rivers by altering water flow, which, in turn, can influence activities along the river (Roynaldi, 2019).

Indonesia, as an archipelagic nation, has extensive coastal waters. The wide sea results in the area having 4 (four) different types of tides, caused by variations in sea depth around these regions (Lee & Chang, 2019). The tides in Indonesia are influenced by coastal topography and tidal waves from the Indian Ocean and the South China Sea (Wei et al., 2016). In addition, river tides are affected by rainfall in a given area (Wang et al., 2019). This has significant implications for ships navigating these rivers. Before embarking on their journeys, crew members must understand tidal patterns to ensure safe, secure navigation (Guerra et al., 2019). This research aims to:
1. Determine the highest tides and lowest tides occurring in the Musi River.
2. Identify the types of tides that occur in the Musi River, specifically the HHWL and LLWL.
3. Forecast the tidal patterns expected in December 2026.

Consequently, it is hoped that this research will be beneficial to ships engaged in navigation. This includes providing insights into the dimensions of ships operating on the river and the allowable cargo height for ships passing under bridges spanning the

Musi River, which are essential for safe navigation. Furthermore, this study serves as a reference for future research concerning the safety of ships involved in the distribution of goods and passengers utilizing the Musi River.

LITERATURE REVIEW

Tidal fluctuations are monitored by observing the water surface over 29 days (Hendri et al., 2019; Mustain, 2021). The tides in rivers are influenced by gravitational forces of the moon and the sun (Finkl & Makowski, 2019; Hendri et al., 2019; Mustain, 2021). Additionally, weather conditions in the region also play a significant role in these tidal variations (Wang et al., 2019). The highest and lowest tides can be determined using monthly data collected during the survey period (Doulgeris et al., 2024).
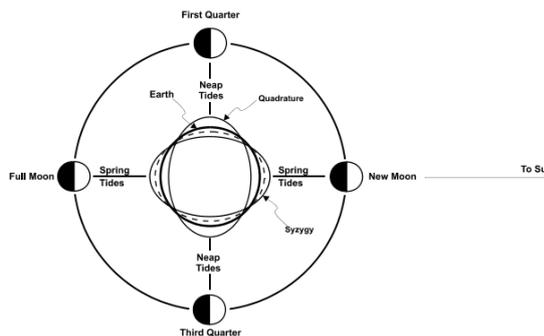

Figure 1. Tidal Illustration

The characteristics of tidal patterns in rivers can be categorized into 4 four types (Hendri et al., 2019). One of them is the semi-diurnal tide, observed in a significant majority of rivers worldwide, particularly those near the sea (Pugh, 2004). This type is characterized by two high tides and two low tides occurring within a single lunar day. Another type is the diurnal tide, where the river experiences only one high tide and one low tide each lunar day. In this tidal pattern, the river water typically contains a measurable amount of salt (Geyer & MacCready, 2014). Other types are mixed prevailing semi-diurnal and mixed prevailing diurnal tides. In this category, the tidal cycles can vary, with high and low tides occurring one to two times within different time frames (Lee & Chang, 2019). This is a picture of the types of tides that occur in the rivers of the world
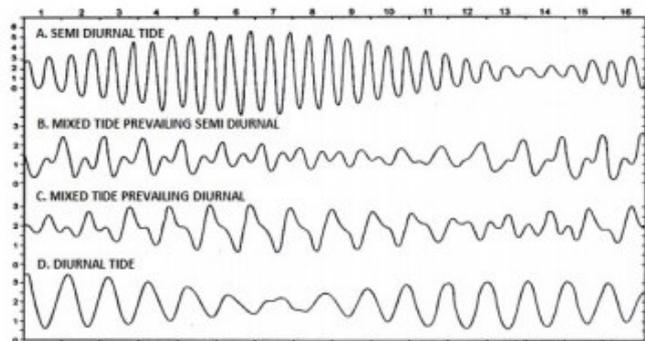
Figure 2. Tidal Types

The Admiralty Method is one of the techniques employed for tidal analysis. This method involves observing tidal over a period of 29 days with hourly intervals (Prayogo, 2021; Mutaqin & Ningsih, 2023; Wahid & Mustakin, 2025). The Admiralty Method is particularly suitable for determining the type of tides in a specific water area due to its high accuracy (Alajuri et al., 2024). In the context of tidal determination, the Admiralty Method is utilized to establish both the Highest High Water Level (HHWL) and the

Lowest Low Water Level (LLWL) (Hoseini et al., 2022; Tapilatu et al., 2023). When conducting an analysis using the Admiralty Method, it is essential to determine the Formzahl number, a critical component for identifying the type of tides. The Formzahl number is established based on the analytical stages derived from calculations using the Admiralty Method (Hendri et al., 2019). The following is the formula used to determine the Formzahl number (Koesuma & Chrismiantari, 2020; Alajuri et al., 2024).

$$F = \frac{(O1 + K1)}{(M2 + S2)}$$

Where :
F : Formzahl Numbers (F<0.25 = semi diurnal tide; 0.25<F≤1/5 = mixed prevailing semi diurnal; 1.5<F≤3.0 = mixed prevailing diurnal; F>3.0 = diurnal
K1 : Magnitude of a Primary Tidal Element (Gravitational Influence of the Sun)
O1 : Magnitude of a Primary Tidal Element (Gravitational Influence of the Moon)
M2 : Magnitude of the Principal Double Tidal Component (Gravitational Influence of the Moon)
S2 : Magnitude of the Principal Double Tidal Component (Gravitational Influence of the Sun)

RESEARCH METHOD

This research was conducted in the Musi River of Palembang City, Indonesia, specifically at the coordinates Latitude -2.99370355150 and longitude 104.7587613120. Data processing involved recording the depth position relative to Mean Sea Level (MSL). The measurement of the water surface elevation was carried out using an Automatic Water Level Recorder (AWLR) published by Balai Besar Wilayah Sungai (BBWS) Sumatera VIII. The AWLR is positioned at a height of 1 meter above MSL datum.

(a)

(b)

Figure 3. (a) Research Location, (b) AWLR Location

Here are the steps undertaken in this research: (1) Data collection of tidal fluctuations was conducted using the Automatic Water Level Recorder (AWLR) owned by the BBWS (Balai Besar Wilayah Sungai) Sumatera VIII over a period of 29 days, from September 19, 2025, to October 17, 2025. Observations were made continuously for 24 hours with a one-hour time interval. The data was recorded using Google Sheets, with the source of information obtained from the BBWS Sumatera VIII website; (2) The data collected over the 29 days was transferred into Microsoft Excel, followed by a recapitulation of the tidal data at the MSL position; (3) An analysis was performed using the Admiralty method, which involved calculations to obtain the values of A and g; (4)

Further analysis was conducted to determine the HHWL, MSL, and LLWL by inputting the variables A and g into the Admiralty method formulas; (5) An analysis was performed to calculate the Formzahl Numbers and to determine the type of tidal pattern in the Musi River; (6) Finally, tidal forecast was carried out using the Admiralty method for December 2026 by incorporating the variables A and g.
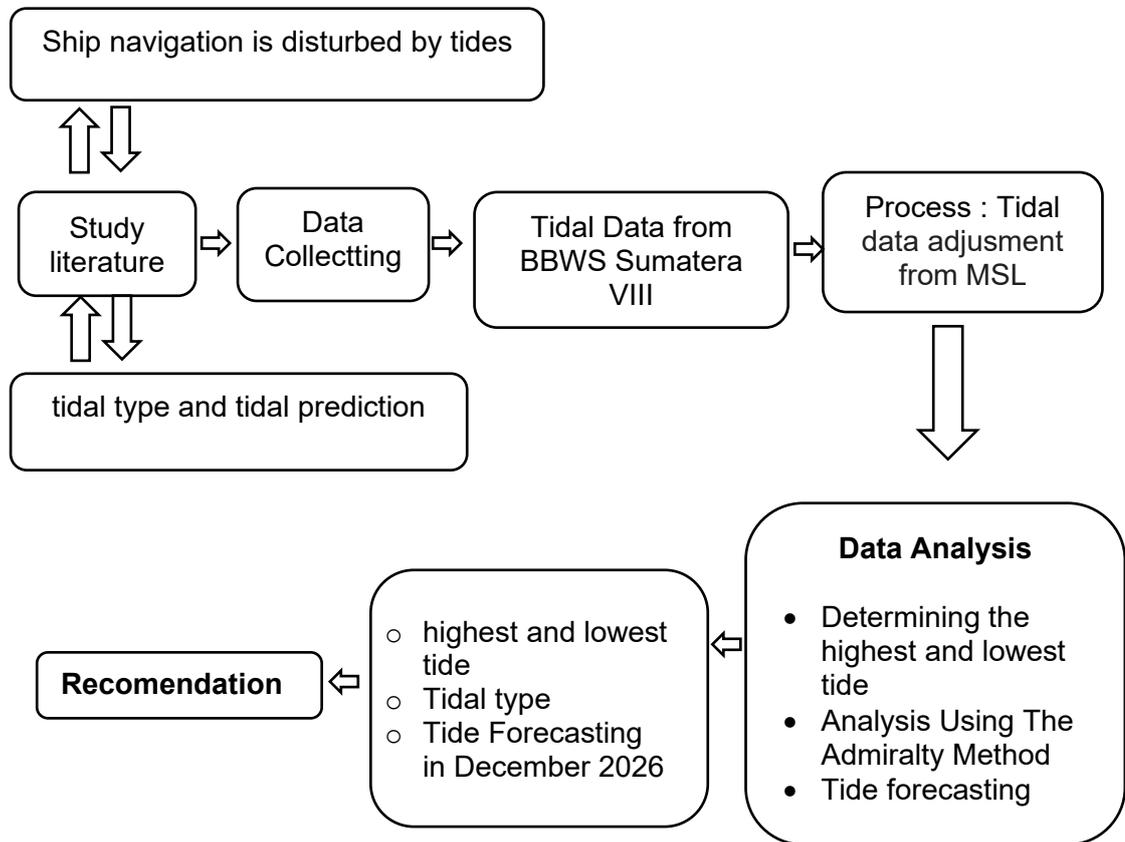

Figure 4. Research Flow Diagram

RESULTS

Below are the data on Water Level Heights obtained from the observations.
Table 1. Tidal Information in the research location

Time	0:55	1:55	2:55	3:55	4:55	5:55	6:55	7:55	8:55	9:55	10:55	11:55	12:55	13:55	14:55	15:55	16:55	17:55	18:55	19:55	20:55	21:55	22:55	23:55
Date													depth (cm)											
19	421	412	393	380	372	360	343	339	325	315	301	292	287	282	274	261	276	343	436	465	477	477	468	447
20	427	421	395	389	377	367	351	338	331	322	314	309	298	293	291	310	352	349	427	452	468	468	468	451
21	435	414	412	384	338	354	355	336	328	319	317	308	310	307	296	292	314	363	394	425	447	460	456	445
22	428	416	401	548	368	352	344	334	338	338	331	324	318	307	299	296	292	319	355	391	419	434	446	433
23	417	395	550	549	352	343	328	329	350	356	359	347	338	330	318	309	298	294	309	352	548	408	548	550
24	391	550	363	347	342	312	309	311	343	370	373	377	373	371	363	352	350	348	348	332	342	361	368	361
25	354	339	327	321	296	288	289	297	332	550	548	549	548	548	547	548	349	338	328	318	335	340	337	326

Time	0:55	1:55	2:55	3:55	4:55	5:55	6:55	7:55	8:55	9:55	10:55	11:55	12:55	13:55	14:55	15:55	16:55	17:55	18:55	19:55	20:55	21:55	22:55	23:55
Date	depth (cm)																							
26	326	317	302	287	276	259	263	272	310	346	548	315	375	412	398	368	357	349	339	321	316	326	322	318
27	311	301	290	278	267	262	253	264	301	340	374	549	418	408	418	414	394	386	375	358	344	336	330	317
28	310	296	277	278	268	264	263	267	298	334	357	388	549	426	431	434	416	403	392	375	356	328	329	323
29	309	291	280	267	251	245	248	250	244	274	310	344	366	394	548	549	421	415	322	379	368	352	338	323
30	308	294	279	266	253	239	229	215	225	257	285	327	361	394	416	423	431	441	430	421	401	392	376	362
01	346	324	310	293	280	260	251	251	245	260	218	324	358	391	412	438	453	454	458	446	431	417	393	550
02	370	350	336	323	307	292	280	268	265	266	269	303	337	550	403	431	445	463	468	466	450	431	419	405
03	391	368	357	343	329	318	305	307	276	265	267	273	293	332	359	377	430	453	457	463	467	449	430	420
04	402	387	368	353	341	326	317	306	291	288	283	277	278	297	328	368	403	431	454	463	469	462	441	276
05	406	396	385	366	353	342	331	318	314	304	299	292	285	285	300	336	372	407	420	437	459	461	462	429
06	413	549	384	364	353	344	335	331	323	314	311	301	296	288	289	300	325	371	549	424	444	443	435	419
07	549	387	550	361	343	336	333	341	347	348	342	336	332	306	306	300	296	313	344	387	549	414	408	549
08	399	373	359	342	331	325	322	340	375	384	380	370	364	337	336	331	312	308	319	343	375	549	384	379
09	372	349	331	325	313	297	296	314	364	548	414	384	409	391	380	360	345	335	327	326	350	352	347	339
10	331	317	301	289	277	269	284	317	364	396	549	549	443	417	548	396	387	371	349	341	330	327	323	313
11	303	300	295	280	264	259	259	281	328	364	548	426	444	453	447	309	262	322	382	371	353	345	327	317
12	305	292	280	267	264	248	244	245	296	332	549	410	435	454	465	464	451	551	549	547	547	548	354	343
13	331	321	301	286	274	260	252	243	261	306	340	549	548	549	549	548	467	448	449	426	411	389	379	359
14	347	331	316	300	286	272	264	241	243	261	308	344	544	416	437	456	466	474	468	451	433	417	398	385
15	371	345	332	317	304	289	275	262	255	254	278	320	359	548	354	440	460	465	471	463	445	364	416	400
16	548	361	343	329	316	304	289	275	262	269	259	323	342	378	400	425	431	459	468	466	455	427	423	548
17	389	549	349	339	320	305	294	287	267	262	262	264	287	322	354	548	337	431	450	458	453	435	544	549

DISCUSSION

For the highest and Minimum Tide, it is possible to calculate the tidal range that occurred during the observation period.

Tidal Range = Highest Tide – Lowest Tide
= 551 cm – 215 cm
Tidal Range = 336 cm

Based on the survey results, the tidal range observed in the Musi River is 336 cm. This tidal range affects ships navigating the Musi River, especially their draft and the height of cargo on board.

Tidal Analysis

Based on Table 1, an analysis was conducted to determine the type of tidal pattern occurring in the Musi River using the Admiralty Method. The Admiralty Method is suitable for identifying the tidal type in a specific water body due to its high accuracy in the results it produces (Alajuri et al., 2024). This method involves calculating harmonic tidal constants from observations collected over 29 days (Pasaribu et al., 2022). From the analysis, harmonic tidal constants were derived, including amplitude (A in cm) and

phase lag (g^0). The harmonic constants consist of nine variables: M_2, S_2, N_2, K_1, O_1, $P1$, M_4, MS_4, and K_2. Subsequently, the type of tidal pattern in the river was determined by calculating the Fomzahl number. Below are the results of the analysis conducted using the Admiralty Method.

Table 2. Result Using Admiralty Method

	S_o	M_2	S_2	N_2	K_2	K_1	O_1	P_1	M_4	MS_4
A cm	364.5	29.1	13.0	4.0	3.0	63.2	51.6	20.9	1.7	6.9
G		254.6	349.8	180.0	349.8	214.0	131.0	214.0	44.4	133.7

Based on the analysis results presented in Table 2, the following conclusions have been drawn:
a S_0 = Mean Sea Level in Musi River 364.5 cm
b M_2 = Harmonic constant by the gravitational constant of the moon, with the height of the moon's 29.1 cm and phase 254.6^0
c S_2 = Harmonic constant by the gravitational constant of the sun, with the height of the sun's 13.2 cm and phase 349.8^0
d N_2 = Harmonic constant by changes in the distance 4 cm to the moon and phase 180^0
e K_2 = Harmonic constant by changes in the distance 3 cm to the sun and phase $349. 8^0$
f K_1 = Harmonic constant by the combined gravitational effects of the moon and the sun, 63.2 cm, and phase 214^0
g O_1 = Harmonic constant by the declination of the moon 51.6 cm and phase 131.1^0
h P_1 = Harmonic constant by the declination of the sun 20.9 and phase 214^0
i M_4 = Harmonic constant by the dual effect of M_2 1.7 cm and phase 44.4^0
j M
   S_4 = Harmonic constant by the interaction of M_2 and S_2 with heigh of 6.9 cm and phase 133.7^0

After obtaining the results from Table 2, calculations were conducted to determine the HHWL, MSL, and LLWL. MSL is derived from the calculation of S0, which is 364.5 cm. To determine the HHWL and LLWL, further calculations can be performed.

HHWL $= AS_0 + (AM_2 + AS_2 + AN_2 + AK_1 + AO_1 + AM_4 + AMS_4 + AK_2 + AP_1)$
HHWL $= 557.71$ cm

LLWL $= AS_0 - (AM_2 + AS_2 + AN_2 + AK_1 + AO_1 + AM_4 + AMS_4 + AK_2 + AP_1)$
LLWL $= 171.26$ cm

Based on the calculation results, the HHWL in the Musi River is recorded at 557.71 cm, while the LLWL in the Musi River is measured at 171.26 cm. The HHWL serves as the maximum air draft for ships navigating the Musi River when passing under bridges. On the other hand, the LLWL can serve as a guideline for the maximum draft of vessels that can operate in the Musi River.

To determine the type of tidal pattern, one must first calculate the Formzhal number.

$$F = \frac{(O1 + K1)}{(M2 + S2)}$$
$$F = \frac{(51.6 + 63.2)}{(29.1 + 13.0)}$$
F = 2.73

Based on the calculations of the formzahl number, it has been determined that a formzahl value of 2.73 indicates that the Musi River is a mixed prevailing diurnal tide (1.5 < F ≤ 3.0). This means that within 24 hours, there is typically one high tide and one low tide, or two high tides and two low tides, occurring at different intervals. The classification of mixed prevailing diurnal tides suggests that the Musi River currently experiences unpredictable tidal fluctuations throughout the day (morning, afternoon, and night), requiring ships to navigate the river with caution.

Based on the harmonic constants presented in Table 2 and the formzahl number, it is possible to forecast water levels for the upcoming months. The forecast for the water level in December 2026 indicates a Highest tide of 511.1 cm and a Lowest Tide of 219.3 cm.

Based on the results of the tidal observation conducted over a period of 29 days (from September 19, 2025, to October 17, 2025), an analysis was performed using the Admiralty method. As a result, the following tidal graph has been produced:
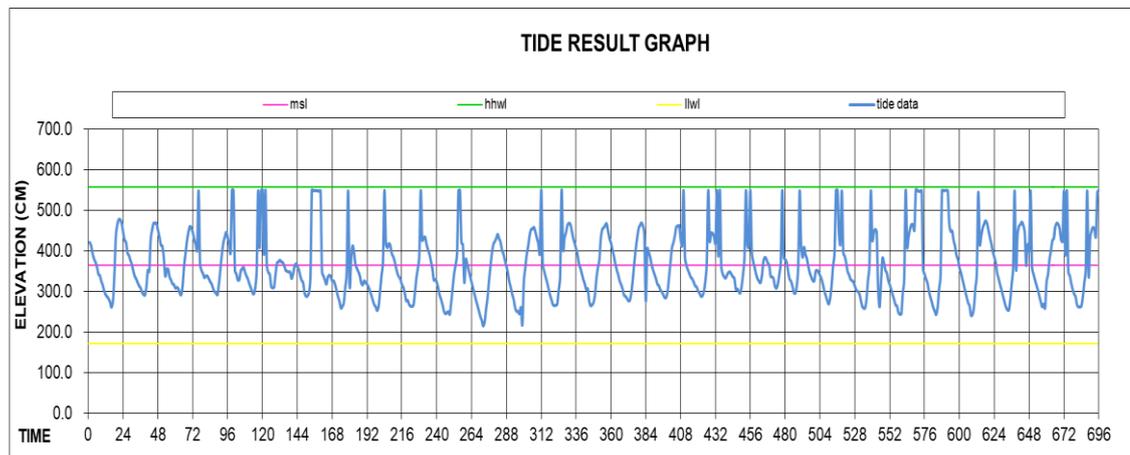

Figure 5. Tide Result Graph

Based on Figure 4, the X-axis (time) represents the time over a 29-day observation period measured in hours, while the Y-axis illustrates the elevation measured in centimeters. From the figure, it can be observed that the HHWL (green line) is at an elevation of 557.71 cm, the LLWL (yellow line) is at an elevation of 171.26 cm, and the MSL (pink line) is at an elevation of 364.5 cm.

The figure shows that the Musi River exhibits a mixed, diurnal tidal pattern. This means that within 24 hours, there are instances of a single high tide, as seen on the 12th day (time 264-288), the 13th day (time 288-312), the 25th day (time 576-600), and the 26th day (time 600-624). However, there are also occurrences of two high and low tides within a single day at different times. This phenomenon is influenced by the significant harmonic constant of the gravitational pull from the moon and the sun, which is measured at 63.2, and is affected by the positions of the moon and the sun relative to the city of Palembang.

Additionally, the following graph compares the tidal data (blue line), HHWL (green line), MSL (pink line), and LLWL (yellow line) with the tidal forecast for December 2026 (red line).
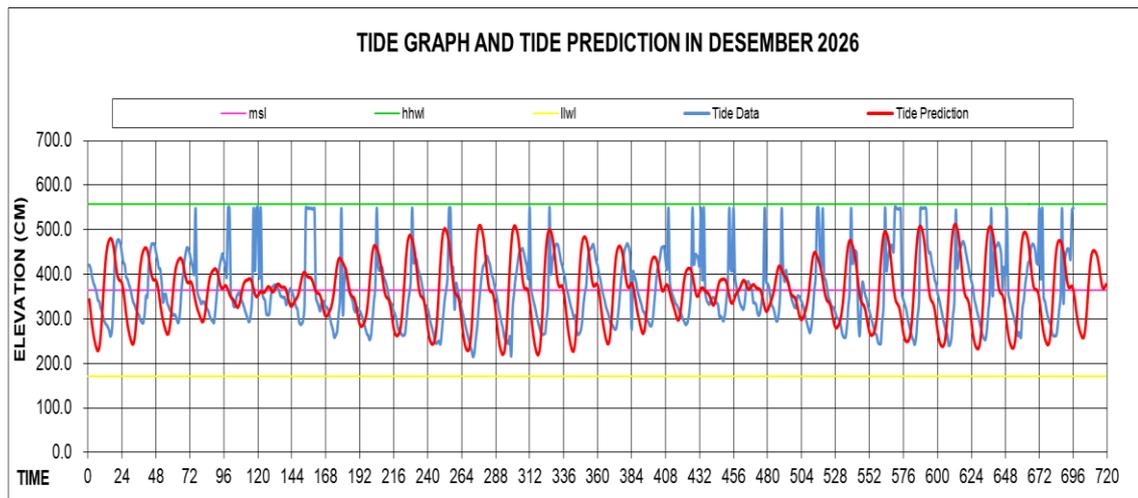
Figure 6. Tide Graph and Tide Prediction in December 2026

Based on Figure 5, the blue line represents Tidal Data of the Musi River, which is classified as a mixed prevailing diurnal type. HHWL is recorded at 557.71 cm, while the LLWL is at 171.26 cm. Furthermore, according to the December 2026 forecast, the highest tide is expected to reach 511.1 cm, and the lowest tide is forecast to be 219.3 cm, resulting in a Tidal Range of 291.9 cm. This change in water level is influenced by climate change and the shallowing of the river in Palembang.

CONCLUSION

Based on the analysis of tidal observations and harmonic calculations in the Musi River waters, several important findings can be described. During the survey period, the highest recorded tide reached 551 cm, while the lowest tide was 215 cm, resulting in a tidal range of 336 cm. This difference in water level indicates that the Musi River experiences significant tidal fluctuations that influence the hydrodynamic conditions of the river.

The tidal characteristics of the Musi River are classified as a mixed prevailing diurnal type, indicated by a form number of 2.73 (1.5 < F ≤ 3.0). This means that within one day the tidal pattern tends to be dominated by one high tide and one low tide, although two tidal events may still occur with unequal heights. The harmonic analysis also shows that the highest high water level (HHWL) reaches 557.71 cm, while the lowest low water level (LLWL) is 171.26 cm. These tidal conditions are strongly influenced by the gravitational forces of the moon and the sun, with a significant harmonic constant value of 63.2. The relative positions of the moon and the sun with respect to the Palembang region also play an important role in shaping the tidal dynamics in the Musi River.

Furthermore, tidal forecasting for December 2026 indicates that the highest tide is expected to reach approximately 511.1 cm, while the lowest tide is predicted to be around 219.3 cm, resulting in a tidal range of about 291.9 cm. The predicted changes in tidal levels may be influenced by several environmental factors, including climate variability and the gradual shallowing of the Musi River due to sedimentation processes in the Palembang area. These conditions highlight the importance of continuous monitoring of tidal dynamics to support navigation safety, river management, and sustainable water resource planning in the Musi River region.

DECLARATION OF CONFLICTING INTERESTS
In the preparation of this scholarly work, the researcher affirms that there are no conflicts of interest that might affect the integrity of the research findings.

REFERENCES

Adalya, N. M., & Mutaqin, B. W. (2022). Modeling of hydro-oceanographic parameters and its possible impact on coral reef cover in Derawan Island waters, East Kalimantan, Indonesia. *Modeling Earth Systems and Environment, 8*(3), 4191–4203.

Alajuri, M. H. S., Kusuma, H. A., Suhendra, T., & Setyono, D. E. D. (2024). Comparison of tidal harmonic based on IoT instrument using Admiralty method in Tanjungpinang waters. *Journal of Applied Geospatial Information, 8*(2), 140–145.

Bedulskis, R. (2023). Legal status of the navigable rivers of the Grand Duchy of Lithuania in the 16th–18th centuries. *Lietuvos istorijos studijos, 51*, 8–21.

Doulgeris, C., Koukouli, P., Georgiou, P., Dalampakis, P., & Karpouzos, D. (2020). Assessment of minimum water level in lakes and reservoirs based on their morphological and hydrological features. *Hydrology, 7*(4), Article 83.

Fathoni, M., Pradono, P., Syabri, I., & Shanty, Y. R. (2017). Analysis to assess potential rivers for cargo transport in Indonesia. *Transportation Research Procedia, 25*, 4544–4559.

Finkl, C. W., & Makowski, C. (2019). Nearshore geomorphological mapping. In C. W. Finkl & C. Makowski (Eds.), *Encyclopedia of coastal science* (pp. 1243–1265). Springer.

Geyer, W. R., & MacCready, P. (2014). The role of tides in the dynamics of estuaries. *Annual Review of Fluid Mechanics, 46*, 1–22.

Guerra, M., Thomson, J., Prusa, T., Falkenhayn Maloy, C., Krembs, C., & Sackmann, B. (2019). Tidal current observations through Admiralty Inlet from ferry-mounted current profilers. *Journal of Ocean Engineering and Marine Energy, 5*(2), 159–172.

Hendri, A., Fauzi, M., Ahmad, R., Ongko, A., & Almanna, F. (2019). The simulation of observation data in predicting tidal patterns using the Admiralty method in Dumai harbour. In *MATEC Web of Conferences* (Vol. 276, Article 04020). EDP Sciences.

Hoseini, S. M., & Soltanpour, M. (2022). Numerical study of influencing factors on tidal wave propagation in the Persian Gulf. *Ocean Science Journal, 57*(4), 642–671.

Isnain, M. N., & Mutaqin, B. W. (2023). Geomorphological and hydro-oceanographic analysis related to the characteristics of marine debris on the south coast of Yogyakarta, Indonesia. *Rendiconti Lincei. Scienze Fisiche e Naturali, 34*(1), 227–239.

Khedr, A. (2024). Sea level analysis for tidal datum realization at Port Tawfik, Suez, Egypt. *Egyptian Journal of Aquatic Biology and Fisheries, 28*(1), 1923–1935.

Koesuma, S., & Chrismiantari, R. V. (2020). Determination of tidal components and tidal types using harmonic analysis in the West Sumatera waters. In *2020 IEEE Asia-Pacific Conference on Geoscience, Electronics and Remote Sensing Technology (AGERS)* (pp. 196–199). IEEE.

Lee, S. H., & Chang, Y. S. (2019). Classification of global tidal types based on auto-correlation analysis. *Ocean Science Journal, 54*(2), 279–286.

Mustain, M. (2021). Simple analysis of determination of tidal types of sea water: A case study in Lamong Bay waters, East Java. In *Proceedings of the 2021 IEEE Ocean Engineering Technology and Innovation Conference (OETIC)* (pp. 13–17).

Mutaqin, B. W., & Ningsih, R. L. (2023). Tidal characteristics in the southern waters of Java, Indonesia. *Jurnal Geografi, 15*(2), 154–164.

Pasaribu, R. P., Sewiko, R., & Arifin, A. (2022). Application of the Admiralty method to process tidal data in the waters of the Nasik Strait Bangka Belitung. *Jurnal Ilmiah PLATAX, 10*(1), 146–160.

Patil, A. R., Lambrechts, J., Draoui, I., Perez, F. F., & Deleersnijder, E. (2024). Numerical modelling of navigable rivers: Influence of navigation structures in the Meuse River flow. In *River Flow 2022* (pp. 647–655). CRC Press.

Prayogo, L. M. (2021). Comparison of Admiralty and least square methods for tidal analysis in Mandangin Island, Sampang Regency, East Java. *Jurnal Perikanan dan Kelautan, 10*(2), 171–181.

Pugh, D. T. (2004). *Tides, surges and mean sea level*. Wiley-Blackwell.

Putranto, D. D. A., & Buchari, E. (2017). Effect of sedimentation volume on productivity and dwelling time of ships at Bom Baru Port. *MATEC Web of Conferences, 138*, 07006. https://doi.org/10.1051/matecconf/201713807006

Roynaldi, A. D. (2019). Estimation of waste generation from tidal flood in North Semarang sub-district. *E3S Web of Conferences, 125*.

Rusdin, A. (2024). Navigation channel evaluation at Donggala fish landing base in Central Sulawesi. *IOP Conference Series: Earth and Environmental Science, 1355*(1), Article 012039.

Rusdin, A., & Yunar, A. (2024). Navigation channel evaluation at Donggala fish landing base in Central Sulawesi. In *IOP Conference Series: Earth and Environmental Science* (Vol. 1355, No. 1, Article 012039). IOP Publishing.

Santos de Lima, L., Silva, F. E. O. E., Dorio Anastácio, P. R., Kolanski, M. M. D. P., Pires Pereira, A. C., Menezes, M. S. R., … Macedo, M. N. (2024). Severe droughts reduce river navigability and isolate communities in the Brazilian Amazon. *Communications Earth & Environment, 5*(1), Article 370.

Sulistiyani, P., Imanudin, M. S., & Said, M. (2019). Sedimentation rate and characteristics of Musi River mud, Palembang City, South Sumatra. *Journal of Wetlands Environmental Management, 7*(1), 95–105.

Tapilatu, M. E., Kaber, Y., Alzair, N., Wona, H., Grady, K. C., & Tapilatu, R. F. (2023). Using remote sensing to evaluate coastal erosion and accretion to guide conservation of turtle nesting sites. *International Journal of Environmental Science and Technology, 20*(6), 7007–7018.

Wahid, N. M., & Mutaqin, B. W. (2024). Tidal fluctuation effect on marine debris characteristics in the Kulon Progo beaches of Yogyakarta, Indonesia. *Journal of Coastal Conservation, 28*(1), Article 37.

Wang, Y., et al. (2019). The effects of climate change on tidal dynamics. *Climatic Change, 155*(1), 1–15.

Wei, Z., Fang, G., Susanto, R. D., Adi, T. R., Fan, B., Setiawan, A., & Gao, X. (2016). Tidal elevation, current, and energy flux in the area between the South China Sea and Java Sea. *Ocean Science, 12*(2), 517–531.